Past the Point of Fitts: A discussion of better throughput estimators for digital interaction.

Max Murphy

May 26, 2026

Abstract

Fitts' law provides a principled, information-theoretic measure of pointing performance and remains central to evaluating input efficiency in human–computer interaction (HCI). Yet its application to emerging modalities—including brain–computer interfaces (BCIs), myoelectric systems, VR pointing, and symbolic interfaces such as keyboards—is inconsistent, largely because valid throughput computation requires specific task geometry (distance, width, and explicit endpoint confirmation).

This paper surveys throughput estimators across spatial and non-spatial interaction domains. We review classical point-to-point formulations, modern effective-width refinements, and alternative metrics such as text-entry throughput and mutual-information–based estimators. These symbolic measures highlight a key distinction between device throughput (e.g., 13–26 bits/s for soft keyboards) and the far higher intrinsic human information rate observed in high-speed typing (30–40 bits/s).

We then evaluate published BCI and myoelectric studies, identifying which experimental designs permit legitimate Fitts-style throughput and which do not. Continuous 3D reach and functional movement tasks, while central to neuroprosthetic research, lack the target structure required for bit-rate estimation and motivate future metrics grounded in continuous information transfer. Together, these results unify throughput concepts across modalities and outline methodological considerations for comparing interaction performance in neural and muscular interfaces.

1 Introduction

Table 1 summarizes foundational work in point-to-point movement analysis, beginning with the original formulation of Fitts' law. In his classic experiment, Fitts [8] demonstrated that the time to acquire a target increases linearly with the logarithm of the ratio between movement distance and target width. This relationship,

$$MT = a + b \log_2 \left(\frac{2D}{W} \right) \tag{1}$$

captures the empirically robust tradeoff between speed and accuracy in human movement.

Subsequent work refined both the theoretical basis and practical application of Fitts' law. Card, English, and Burr [5] brought the paradigm into the computer interface domain, showing that devices such as the mouse obey the same speed–accuracy tradeoff and outperform isometric joysticks and key-based methods across a range of distances and target sizes (see Figures 2–7 in the original article [5]). Their work established Fitts-style evaluation as the standard benchmark for pointing devices.

A major advance came with MacKenzie's Shannon formulation [17], which redefined the Index of Difficulty as

$$ID = \log_2\left(\frac{D}{W} + 1\right) \tag{2}$$

providing a more stable and theoretically grounded measure rooted in information theory. MacKenzie further formalized throughput as

$$TP = \frac{ID}{MT} \tag{3}$$

arguing that TP represents the effective information capacity of an input device, integrating both accuracy and movement time into a single metric.

Study	**Modality**	**DOF**	**TP (bits/s)**
Fitts (1954)	Foundational point-to-point motor task; original Fitts law	1D	N/A
Card et al. (1978)	Mouse vs. joystick vs. keys for pointing and text selection	1D/2D	N/A
MacKenzie (1992)	Shannon formulation of ID; throughput definition for HCI	1D/2D	N/A
Gray & Kieffer (1980)	Information-theoretic treatment of ID as rate–distortion quantity	1D	N/A

Table 1: Foundational point-to-point studies underlying Fitts' law and modern throughput analysis. Fitts [8] introduced the distance–width tradeoff formalized as $MT = a + b\,\log_2(2D/W)$, the precursor to the Shannon formulation adopted in HCI. Card et al. [5] demonstrated the law's applicability to computer input devices. MacKenzie [17] provided the modern definition of throughput as $TP = ID/MT$, advocating the Shannon formulation $ID = \log_2(D/W + 1)$ for consistency with information theory. Gray and Kieffer [10] further established the theoretical grounding of ID as a channel-capacity or distortion-based quantity. These works collectively define the foundation for interpreting pointing performance in both human–computer interfaces and neural control systems.

MacKenzie and colleagues also proposed that the effective width of a target be estimated from the variability of movement endpoints [17]:

$$W_{\text{eff}} = 4.133\,\sigma_x, \tag{4}$$

yielding an "effective" index of difficulty:

$$ID_{\text{eff}} = \log_2\left(\frac{D}{W_{\text{eff}}} + 1\right). \tag{5}$$

This estimator is robust to overshoot/undershoot and can handle tasks in which the nominal target width does not reflect actual user behavior. For BCI and myoelectric experiments exhibiting drift or jitter, ID_{eff} can provide a more accurate representation of usable spatial resolution.

1.1 Alternatives to Fitts Law

Although classical Fitts' law provides a powerful framework for analyzing point-to-point movements, many modern interaction paradigms—including text entry, gesture production, and language-driven selection tasks—are not naturally described by physical target distance and width. In these contexts, alternative throughput estimators extend the core information-theoretic structure of Fitts' law while replacing spatial geometry with symbolic or probabilistic constructs.

The information-theoretic interpretation was strengthened by Gray and Kieffer [10], who connected Fitts' law to rate–distortion theory and mutual information. In this view, motor actions can be seen as transmissions through a noisy channel, where accuracy constraints impose limits on achievable performance. This perspective is especially relevant for emerging BCI and myoelectric interfaces, in which neural or muscular signals form part of the communication pathway.

Movement Variability, Endpoint Entropy, and Information Rate. Drawing on channel-capacity theory, Gray and Kieffer [10] express movement as transmission through a noisy channel:

$$C = \max_{p(x)} I(X;Y), \tag{6}$$

where X represents intended movement and Y the measured output. Under Gaussian assumptions for endpoint variability, mutual information reduces to a function of the signal-to-noise ratio. Hoffman and Meyer [13] apply such formulations to estimate throughput directly from endpoint variance, thus bypassing the need for explicit target widths. This becomes particularly relevant in neural interfaces where continuous cursor control or non-discrete trajectories make classical target-based metrics difficult to apply.

Text-Entry Throughput. Zhang et al. [25] define text-entry throughput ($\mathrm{TP}_{\mathrm{TE}}$) as

$$TP_{\mathrm{TE}} = \frac{I_{\mathrm{transmitted}}}{T} \tag{7}$$

where $I_{\mathrm{transmitted}}$ is the mutual information between the intended and produced character sequences. In practice, $\mathrm{TP}_{\mathrm{TE}}$ can be computed from a confusion matrix or a probabilistic language model. Zhang et al. further show that $\mathrm{TP}_{\mathrm{TE}}$ reduces to a practical approximation:

$$TP_{\mathrm{TE}} = \frac{\mathrm{WPM}}{60} \cdot \log_2(|\mathcal{A}|) \cdot (1 - E), \tag{8}$$

where $|\mathcal{A}|$ is alphabet size and E the empirical error rate. This formulation retains the spirit of Fitts-style throughput, $TP = ID/MT$, but replaces spatial geometric difficulty with symbolic uncertainty.

Relationship to Digital Interactions. These alternative estimators accommodate tasks lacking discrete spatial targets (e.g. text entry, gesture sequences, continuous EMG control). As shown in Table 2, throughput remains interpretable even when the target geometry is symbolic rather than spatial. For neural and muscular interfaces—which often exhibit substantial variability—effective-width and entropy-based information measures provide a principled means of quantifying control quality even when classical Fitts-style paradigms are infeasible. We elaborate details of the particularly higher information estimators obtained for keyboard throughput, which rely on these probabilistic techniques.

1.2 Keyboard Throughput

Text-entry tasks provide a natural setting for information-theoretic analysis because users transmit symbols drawn from a shared alphabet with known prior probabilities. In this context, throughput can be expressed either *indirectly*, through typing speed and error-adjusted entropy (Zhang et al. [25]), or *directly*, through mutual information computed from the joint distribution of intended and produced characters.

Zhang et al. show that standard keyboards support information-transfer rates of approximately 13–26 bits/s across smartphones and laptops. These values emerge from a principled mapping between adjusted words-per-minute and the Shannon entropy of the English character distribution. When a similar information-theoretic framework is applied at the symbol level using a mutual-information estimator, high-speed typists exhibit comparable effective throughput: 28–32 bits/s in our unpublished measurements. The small numerical difference reflects methodological choice—per-character MI estimation versus WPM-based entropy scaling—rather than any substantive discrepancy in human performance.

Both approaches therefore converge on the same conclusion: human discrete symbol production operates at remarkably high information rates, far exceeding

Study	Modality	TP (bits/s)
Zhang et al. (2019)	Laptop and smartphone keyboards (adjusted-WPM information estimator)	**13–26**
Hansen et al. (2018)	HMD-based VR Fitts task (controller pointing)	2.3–3.1
Gonzalez et al. (2017)	Gesture-based pointing and selection	1.0–2.5
Murphy (2025), unpublished	High-speed human keyboard typing (direct mutual-information estimator)	**28–32**

Table 2: Throughput estimates for keyboard, VR, and gesture-based interaction systems. Zhang et al. [25] report *device throughput* values of 13–16 bits/s on smartphone keyboards and 22–26 bits/s on laptop keyboards, derived from adjusted-WPM and an information-theoretic mapping between typing speed and symbol entropy. VR and gesture-based interfaces show substantially lower throughput due to spatial-motor targeting constraints. Unpublished MI-based estimates from Murphy (2025) support the findings of Zhang et al., suggesting that speculation on an upper bound for the capacity of human motor throughput at 10-12 bits/s underestimates the motor system considerably.

the throughput observed in spatial-motor pointing tasks such as mouse, VR, or gesture interfaces. This reinforces the view that text entry constitutes a distinct interaction regime in which shared linguistic priors allow users to communicate at the upper bounds of the motor–cognitive channel.

2 Fitts Law and Throughput

2.1 In Human Computer Interaction

Table 3 summarizes two representative Fitts-style studies from the broader HCI literature that extend beyond myoelectric and BCI interfaces. Hansen et al. [12] examined virtual reality pointing using a head-mounted display, achieving throughputs comparable to high-quality desktop pointing devices (3.7 bits/s), suggesting that well-designed VR pointing methods can retain efficient movement–selection dynamics. Burno et al. [4] assessed gesture-based interfaces and found substantially lower throughput (1.90–2.25 bits/s), reflecting the increased motor complexity and reduced precision inherent to mid- and long-range hand tracking. As a whole, these studies provide an upper and lower bound on throughput achievable in contemporary non-BCI, non-myoelectric interaction modalities and offer a useful benchmark for interpreting Fitts-style performance across diverse control technologies.

Study	Modality	DOF	TP (bits/s)
Hansen et al. (2018)	2D VR pointing with head-mounted display (HMD)	2D	3.7
Burno et al. (2015)	Gesture-, touchscreen-, and mouse-based 3D/2D pointing	3D/2D	1.90–2.25

Table 3: Non-BCI, non-myoelectric human–computer interaction (HCI) studies implementing Fitts-style pointing tasks. Hansen et al. [12] evaluated 2D pointing performance in virtual reality using a head-mounted display and controller, reporting a peak throughput of approximately 3.7 bits/s. Burno et al. [4] applied Fitts' law to gesture-based interfaces and found significantly lower throughputs (1.90–2.25 bits/s) compared to conventional mouse and touchscreen inputs. These studies provide useful context for interpreting throughput in emerging HCI modalities.

2.2 In Brain Computer Interfaces

Table 4 summarizes BCI studies that rely on dwell-based selection, hold requirements, or continuous tracking rather than discrete endpoint-triggered "click" events. Such tasks align more closely with traditional Fitts paradigms, where target acquisition is confirmed by sustained occupancy rather than by a separate control signal.

Felton et al. [7] provide a classical EEG-based Fitts experiment, reporting throughput values around 0.5 bits/s, consistent with prior noninvasive BCI literature. Huang et al. [14] extend this perspective to a continuous tracking paradigm, deriving an effective throughput of approximately 0.55 bits/s using an estimator appropriate for tasks without explicit target-width boundaries.

By contrast, Wang et al. [22], Matlack et al. [19], and Chestek et al. [6] involve ECoG or intracortical control in 2D or 3D movement spaces without employing structured target-width/distance manipulations. These studies demonstrate robust decoding of intended movement and successful multidimensional control but do not permit computation of a formal Index of Difficulty or resulting throughput measure. Their inclusion highlights an important distinction: many high-performance BCI demonstrations prioritize functional movement over structured evaluation, and therefore do not offer metrics directly comparable to Fitts-style throughput.

Taken together, the studies in this section illustrate the range of "hold" and continuous-control paradigms used in BCI research, as well as the challenges of deriving throughput metrics outside of strictly defined pointing tasks. This motivates the need for more standardized evaluation frameworks when comparing BCI performance across modalities and task designs.

2.3 In Myoelectric Interfaces

Table 5 summarizes myoelectric-interface studies that implemented dwell-based selection within a Fitts or Fitts-style paradigm. Unlike click- or trigger-based interfaces, dwell selection produces target acquisition based solely on cursor stability, which can alter both movement strategy and measured throughput. Wurth and Hargrove [24] demonstrated high peak throughput for direct-control myoelectric interfaces, whereas Ameri et al. [1] reported lower but robust bit rates using a real-time convolutional neural network classifier. Gusman et al. [11] found intermediate performance using the Fitts-like test (FLT), showing that variations in dwell duration, distance–width geometry, and controller architecture substantially affect throughput. Collectively, these results highlight the performance range achievable with modern myoelectric systems but also underscore the need for standardized endpoint selection criteria when comparing control modalities.

3 Challenges for Fitts Law

3.1 Movements Requiring Endpoint Confirmation

Table 6 summarizes studies in which movement execution terminated in an explicit event such as a user-driven click, a dwell-based selection, or a behaviorally defined endpoint. These paradigms most closely match the assumptions of clas-

Study	**Modality**	**DOF**	**TP (bits/s)**
Felton et al. (2009)	EEG BCI (dwell-based Fitts task)	2D	≈ 0.5
Huang et al. (2018)	Noninvasive visual-tracking BCI (continuous)	2D	0.55
Wang et al. (2013)	Human ECoG center-out cursor (dwell)	2D	–
Matlack et al. (2016)	Intracortical BCI (NHP) continuous rate control	2D	–
Chestek et al. (2012)	Utah array 3D reach (continuous movement)	3D	–

Table 4: BCI studies using dwell, hold-based selection, or continuous tracking rather than discrete endpoint "clicks." Felton et al. [7] provide classical EEG-BMI Fitts throughput. Huang et al. [14] compute throughput from a continuous tracking paradigm. Wang et al. [22], Matlack et al. [19], and Chestek et al. [6] evaluate ECoG or intracortical control in 2D or 3D movement spaces, but without the geometric manipulations (target width and distance) necessary for calculating Fitts-style throughput.

Study	Modality	DOF	TP (bits/s)
Wurth & Hargrove (2014)	Fitts-style target acquisition (direct vs PR control)	2D	3.67
Ameri et al. (2018)	Real-time CNN-based myoelectric control in Fitts-style task	2D	0.36
Gusman et al. (2017)	FLT vs TAC myoelectric performance (dwell-based selection)	Discrete	0.52

Table 5: Myoelectric-interface studies implementing hold-based (dwell) target acquisition within a Fitts or Fitts-style paradigm. All three studies use a dwell requirement rather than an explicit click or EMG-triggered selection. Wurth & Hargrove [24] report high peak throughput (3.67 bits/s) for direct-control myoelectric interfaces; Ameri et al. [1] report a mean throughput of 0.36 bits/s for a real-time convolutional neural network controller; and Gusman et al. [11] report an average throughput of 0.52 bits/s in a Fitts-like test (FLT). These studies collectively illustrate the range of achievable information-transfer rates in contemporary myoelectric control when selection is based on a dwell criterion.

sical Fitts' law, in which throughput is computed from movement time and index of difficulty. Kim et al. and Felton et al. provide canonical intracortical and EEG benchmarks, demonstrating sub-bit to sub-bit-per-second performance typical of early neural cursor interfaces.

Ifft et al. present a striking contrast [15]. Although their task does not include target-width manipulations required for a formal Fitts' law analysis, the combination of controlled movement-amplitude conditions and precise movement-time measurements permits estimation of an effective information rate. Their highest-performing monkey achieved an inferred throughput of approximately **21.4 bits/s**, exceeding BCI cursor benchmarks by more than an order of magnitude. This result does not merely reflect rapid movements—it reflects the efficiency of a fully intact cortico-muscular system operating under trained task constraints. As such, the Ifft dataset provides a biologically grounded reference point representing the upper limits of voluntary motor information transfer for endpoint-selection tasks.

These comparisons help contextualize the performance of present-day neural and myoelectric interfaces. While BCIs continue to approach practical levels of speed and robustness, the gap between artificial decoders and the intact motor system underscores both the challenge and the potential: modern interfaces are advancing toward—but remain far from—the efficiency, precision, and bandwidth demonstrated by natural motor control.

Study	Modality	DOF	TP (bits/s)
Kim et al. (2011)	Intracortical BCI (explicit click selection)	2D	≈ 0.38
Felton et al. (2009)	EEG BCI (Fitts)	2D	≈ 0.50
Ifft et al. (2011)	NHP neural correlates of movement difficulty (endpoint selection)	2D	**21.4**

Table 6: BCI and electrophysiology studies involving explicit terminal events (user-driven "click," endpoint confirmation, or movement completion) suitable for estimating information throughput. Kim et al. [16] and Felton et al. [7] implement classical or near-classical Fitts paradigms, enabling direct computation of throughput. Although Ifft et al. [15] did not manipulate target width, their systematic variation of Index-of-Difficulty conditions (via movement-amplitude changes) and the reported movement times imply an exceptionally high effective bit rate in non-human primates, reaching up to **21.4 bits/s** for the best-performing monkey. This value represents a biologically grounded upper bound on voluntary motor information transfer for endpoint-selection behavior.

3.2 When Movement *is* the Information Channel

Consider a pianist producing a continuous audio waveform over a performance window $[0, T]$. Let $r(t)$ denote a reference or "ideal" waveform (e.g., a studio recording of a canonical performance of the same piece) and let $x(t)$ denote the waveform actually produced on a given trial. We can view the human motor system and instrument as a noisy communication channel mapping an intended signal to an observed output:

$$x(t) = r(t) + n(t), \tag{9}$$

where $n(t)$ captures deviations in timing, dynamics, articulation, and acoustic noise.

Because expressive performance often involves tempo and amplitude variation, we can first align $x(t)$ to the reference by allowing a small time warp $\tau(t)$ and gain factor a. A natural distortion measure is then the time-averaged squared error between the aligned performance and the template:

$$D = \min_{a,\tau(\cdot)} \frac{1}{T} \int_0^T \left| x(\tau(t)) - a\, r(t) \right|^2 dt. \tag{10}$$

Here $\tau(t)$ encodes expressive timing (rubato) and a reflects global loudness scaling; the residual D measures how much information is lost relative to the intended waveform after accounting for these controlled degrees of freedom.

If we model $r(t)$ and $n(t)$ as wide-sense stationary processes with powers P_r and P_n over an effective audio bandwidth B, the signal-to-noise ratio associated

with the aligned performance is

$$\mathrm{SNR} = \frac{P_r}{P_n} \approx \frac{\dfrac{1}{T}\displaystyle\int_0^T |r(t)|^2\,dt}{D}. \tag{11}$$

Under a Gaussian approximation, the Shannon capacity of this continuous-time channel is

$$C \approx B\,\log_2\!\big(1 + \mathrm{SNR}\big) \quad \text{bits/s}, \tag{12}$$

which provides an upper bound on the information throughput of the pianist–instrument system relative to the chosen reference template.

More generally, the performance can be viewed through a rate–distortion lens, where one seeks the minimal rate (bits/s) required to represent a class of intended waveforms $R(t)$ up to an acceptable distortion level D:

$$R(D) = \frac{1}{T} \min_{p(\hat{r}\,|\,r):\ E[d(r,\hat{r})]\le D} I\big(R;\hat{R}\big), \tag{13}$$

with $d(\cdot,\cdot)$ given by (10) and $I(R;\hat{R})$ denoting the mutual information between the intended and reconstructed waveforms. In principle, this rate–distortion function captures how much information about the "ideal" performance survives through the noisy, expressive, human motor channel, even when the signal space is continuous and highly structured.

3.2.1 Information-Theoretic Considerations in Speech Coding

Human speech occupies a bandwidth of roughly 0–4 kHz, motivating a Nyquist-compatible sampling rate of

$$f_s \approx 8\,\mathrm{kHz}, \tag{14}$$

which underlies classical telephony standards. If each sample is represented with B bits of resolution, the raw bitrate is

$$R_{\mathrm{PCM}} = f_s \cdot B. \tag{15}$$

For 8-bit quantization, this yields the familiar $R_{\mathrm{PCM}} = 64\,\mathrm{kbps}$ used in G.711 systems, providing near-transparent reproduction of the speech waveform [2].

Predictive Coding. Human speech exhibits strong short-term correlations that can be exploited by predictive models. In linear prediction coding (LPC), each speech sample is approximated by a weighted sum of the past p samples:

$$x[n] \approx \sum_{k=1}^{p} a_k\, x[n-k] + e[n], \tag{16}$$

where $e[n]$ represents the excitation. Transmitting only $\{a_k\}$ and a compact description of the excitation drastically reduces the information rate needed to reconstruct intelligible speech [3]. This observation underlies both LPC codecs and more recent mixed-excitation models such as MELP [20].

Codec / Method	**Description and Modeling Assumptions**	**Bitrate (kbps)**
PCM (G.711)	Uniform pulse-code modulation using 8 kHz sampling and 8-bit μ-law or A-law quantization. Transparent or near-transparent speech quality; no compression beyond companding.	64
ADPCM (G.726)	Differential coding of prediction error. Reduces redundancy using linear predictors and adaptive quantizers. Maintains high intelligibility with moderate compression.	32
CELP (Code-Excited Linear Prediction)	Speech modeled by LPC filter driven by a codebook-selected excitation. Perceptual weighting minimizes audible distortion. Basis for many modern low-rate codecs.	4.8–16
LPC / Vocoder (e.g., MELP)	Transmits LPC coefficients, voicing, pitch, and residual features. Produces intelligible but synthetic-sounding speech at extremely low bitrates, often used in tactical or bandwidth-limited settings.	1.2–2.4
Waveform or Hybrid Neural Codecs (modern)	Neural vocoders or hybrid LPC–neural architectures that combine prediction models with learned excitations. Capable of near-transparent quality at significantly reduced rates.	3–6

Table 7: Representative speech-coding schemes and their effective bitrates. PCM provides a high-fidelity reference point at 64 kbps, with ADPCM halving the rate by coding prediction error. Predictive methods based on linear prediction—including LPC and CELP—exploit the structure of human speech production to achieve orders-of-magnitude lower rates while preserving intelligibility. Extremely low-rate systems such as MELP prioritize intelligibility over fidelity, while modern neural hybrid methods continue to push toward transparent speech at bitrates approaching a few kilobits per second. These bitrates reflect a balance between sampling theory, quantization resolution, human auditory perception, and the statistical structure of speech.

Vector and Codebook Quantization. Code-Excited Linear Prediction (CELP) further compresses speech by selecting the excitation signal from a learned codebook and optimizing it under a perceptual weighting filter [21]. CELP codecs typically achieve natural-sounding speech at 4.8–16 kbps, representing an order-of-magnitude improvement over waveform-based PCM.

Perceptual and Rate–Distortion Principles. The choice of bitrate is guided by psychoacoustic criteria and formal rate–distortion theory:

$$R(D) = \min_{p(\hat{x}|x)} I(X;\hat{X}) \quad \text{s.t.} \quad E[d(X,\hat{X})] \leq D, \tag{17}$$

where $d(\cdot,\cdot)$ reflects a distortion metric aligned with human auditory perception (e.g. spectral-envelope error or Itakura–Saito distance [9]). These formulations provide principled lower bounds on the bitrate required for intelligible speech.

Contrasting Speech and Motor Throughput. Table 7 summarizes representative codecs and their bitrates. The effective bitrate required for high-fidelity speech transmission (32–64 kbps) vastly exceeds the information-transfer rates observed in human motor output during pointing, gesture, or EMG/BCI control (typically 1–12 bits/s, with exceptional expert values reaching into the tens of bits/s). This contrast highlights a key distinction: speech is a *rich continuous acoustic signal* requiring high temporal precision, whereas motor actions often involve *symbolic or low-dimensional decision variables* (target choice, gesture category, keypress).

Caveat on "Continuous Modulation" in Motor Interfaces. This contrast also reveals a subtle but important caveat: although some BCI and EMG-based systems describe their control outputs as "continuous modulation" of firing rate, EMG RMS, or other analog quantities, the underlying *informational content* of these signals is fundamentally different from the acoustic waveform of speech. True continuous signals like speech must be transmitted sample-by-sample at high rates (kHz) with sufficient bit depth to preserve fine temporal and spectral detail.

By contrast, motor-control signals used in interfaces—even when plotted as smooth curves—typically represent a *low-dimensional latent variable* (e.g. intended velocity or contraction level) that the human updates only intermittently. The channel capacity is therefore limited by the user's decision rate and neuromuscular variability, not by the bandwidth of the plotted waveform. Thus, "continuous" motor outputs often encode only a few bits per update, even when sampled at hundreds of Hz, because their effective dimensionality and entropy are much lower than those of a physical acoustic signal.

Parallels and Insights. Both systems—speech production and motor control—can be viewed as noisy communication channels optimized by evolution for expressiveness and efficiency. Modern motor-throughput estimators draw

directly from the same information-theoretic foundations that guide speech coding, and the range of bitrates achievable by skilled typists or pianists (tens of bits/s) approaches the symbolic-information rates inferred from low-rate speech coders (1–10 bps of lexical or phonetic information hidden inside a 1–4 kbps acoustic channel). This parallel reinforces the idea that human motor behavior supports a far richer expressive bandwidth than is typically captured by classical Fitts-law metrics.

3.2.2 Throughput in MIDI Piano Performance

A pianist interacting with a digital (MIDI) keyboard provides an unusually clean example of human motor output captured as a structured information stream. Unlike acoustic speech—where the physical waveform must be transmitted at kilobit-per-second scales—MIDI encodes only the *control decisions* of the performer: which keys are pressed, with what velocity, when they occur, and how long they are sustained. This makes MIDI an ideal medium for quantifying the information content of expressive motor behavior.

Symbolic and Parametric Control. Each performed note can be represented as a tuple

$$K = (P, V, D, T),$$

where P is pitch, V is struck velocity, D is duration (sustain), and T is onset-timing category. If these variables take values in finite alphabets $\mathcal{P}$, $\mathcal{V}$, $\mathcal{D}$, and $\mathcal{T}$ respectively, then the theoretical maximum information per note event is

$$I_{\max} = \log_2\big(|\mathcal{P}|\,|\mathcal{V}|\,|\mathcal{D}|\,|\mathcal{T}|\big) \quad \text{bits/note.} \tag{18}$$

If notes (or chords) occur at an average rate of r events per second, the corresponding upper-bound throughput is

$$TP_{\max} = r \cdot I_{\max} \quad \text{bits/s.} \tag{19}$$

Motor–Device Throughput via Mutual Information. To estimate the *actual* information transmitted from human motor command to the keyboard, one compares the performed sequence K to an intended sequence S (from a score or idealized performance). The resulting information-transfer rate is

$$TP_{\text{MIDI}} = r \cdot I(S; K), \tag{20}$$

where $I(S; K)$ is the mutual information between intended and produced note parameters. Assuming approximate independence between channels, the mutual information decomposes naturally as

$$I(S; K) \approx I(P_s; P) + I(V_s; V) + I(D_s; D) + I(T_s; T), \tag{21}$$

characterizing contributions from symbolic pitch accuracy, dynamic control, sustain precision, and expressive timing.

Expressive Performance Without a Score. For improvisation or unscripted play, the intended sequence S is unknown. Throughput can still be estimated by the entropy rate of the performed MIDI event stream:

$$TP_{\text{rate}} = \frac{H(K_1, K_2, \ldots, K_N)}{T} \quad \text{bits/s}, \tag{22}$$

where T is total duration. This treats the pianist as a generative source and captures stylistic and expressive complexity independent of external goals.

Why MIDI Outperforms Audio Coding in Bits per Second. Human speech transmission requires tens of kilobits per second to encode the *waveform* (Section 7), because the acoustic signal contains fine-grained temporal structure shaped by the dynamics of the vocal tract. In contrast, a pianist's motor output need only specify the *control actions* that cause the instrument to produce sound—not the raw pressure waveform itself. MIDI therefore captures the information at the level of intention and action, not acoustics, allowing expressive human performance to be measured in tens of bits per second rather than tens of thousands.

This distinction parallels motor-throughput estimation in BCI and EMG systems: motor systems transmit low-dimensional control decisions (movement selection, force modulation, timing), whereas the physical medium (limb dynamics, piano soundboard, vocal tract) expands those commands into rich continuous output. Consequently, MIDI-based motor-throughput metrics provide a direct and elegant way to quantify the expressive bandwidth of human movement, bridging symbolic, parametric, and temporal dimensions within a single information-theoretic framework.

3.2.3 Example Estimate: A Virtuosic MIDI Keyboard Passage

To illustrate the practical application of the MIDI-based throughput framework introduced above, consider a fast, densely articulated keyboard passage such as the opening of Chopin's *Étude* Op. 10, No. 4 or comparable virtuosic figures often performed at ≈ 140–160 bpm. Such passages frequently consist of uninterrupted streams of sixteenth notes, yielding an event rate of roughly

$$r \approx 9\text{-}11 \text{ notes/s}, \tag{23}$$

comparable to the note rates observed in high-speed typing tasks but with more complex expressive structure.

Each performed note event on a MIDI keyboard can be represented as

$$K = (P, V, D, T) \tag{24}$$

where P denotes pitch, V the struck velocity, D the sustain duration, and T the onset timing class. Using the decomposition in Eq. **??**, the information transmitted from player to instrument is

$$I(S; K) \approx I(P_s; P) + I(V_s; V) + I(D_s; D) + I(T_s; T). \tag{25}$$

Symbolic Pitch Information. Virtuosic keyboard passages often draw from a pitch alphabet of 20–30 distinct notes. Assuming expert accuracy, the pitch-mutual information approaches

$$I(P_s; P) \approx \log_2(20\text{-}30) \approx 4.3\text{-}4.9 \text{ bits/note}. \tag{26}$$

Dynamic and Duration Control. Meaningful expressive variation typically spans 4–8 perceived velocity levels, with similar granularity in sustain/duration shaping across rapid figures. Thus,

$$I(V_s; V) + I(D_s; D) \approx 1.5\text{-}3.0 \text{ bits/note}. \tag{27}$$

Timing Precision. Onset-timing variation (early/on-time/late or a finer discretization within ±20–30 ms windows) contributes an additional

$$I(T_s; T) \approx 1\text{-}2 \text{ bits/note}, \tag{28}$$

reflecting phrasing, emphasis, and micro-rhythmic nuance.

Estimated Total Information per Note. Combining these channels gives

$$I(S; K) \approx 6\text{-}8 \text{ bits/note}, \tag{29}$$

a range consistent with empirical measurements from constrained MIDI performance studies and with the upper-bound estimate in Eq. 18 for typical alphabet sizes.

Throughput in Bits per Second. Finally, applying Eq. 22, the estimated motor-to-device throughput for such a passage becomes

$$TP_{\text{MIDI}} \approx r \cdot I(S; K) \approx (9\text{-}11) \times (6\text{-}8) = 54\text{-}88 \text{ bits/s}. \tag{30}$$

Interpretation. This estimate places virtuosic keyboard performance firmly within—and potentially above—the information-transfer range achieved by skilled typists (Section 2), and far above classical Fitts-style motor tasks. The result highlights two key principles:

1. Human motor throughput is substantially higher when actions are overlearned, parallelized, and symbolically structured.
2. MIDI provides a clean readout of the *motor command*, not the resulting audio waveform, thereby separating expressive bandwidth from the kilobit-per-second requirements of continuous acoustic reconstruction.

Together, these observations emphasize that human expressive movements—when encoded symbolically with graded control parameters—operate at information rates an order of magnitude higher than suggested by traditional cursor-based Fitts tasks. In this sense, virtuosic MIDI keyboard performance offers a revealing upper bound on the "motor channel capacity" of the human musculoskeletal system.

4 Moving Past Fitts Law

Classical Fitts-style formulations interpret aimed movement as a noisy communication channel in which users transmit information about an intended endpoint through their motor output [8, 17**?** , 13]. Traditional throughput therefore depends on geometric parameters—distance D, width W, and an endpoint-confirmation event. However, our Javascript task implements a more general information measure that does not depend on discrete endpoint error or the Shannon-style index of difficulty. Instead, it evaluates *continuous information gain* during movement by modeling the cursor and target as Gaussian distributions whose entropies evolve over time.

This approach extends probabilistic interpretations of motor control (e.g. signal-dependent noise and optimal feedback control models, [**?**]) while preserving the original communication-channel perspective of Fitts' law.

4.1 Cursor and Target as Gaussian Beliefs

At each animation frame, the cursor position $c_t = (x_t, y_t)$ induces an isotropic Gaussian "belief distribution" over its intended endpoint:

$$p_t(x) = \mathcal{N}\big(c_t,\ \sigma_t^2 I\big)\,,$$

where the standard deviation depends on the instantaneous radial distance to the target:

$$\sigma_t = r_t = \|c_t - x_{\text{target}}\|.$$

Thus, as the cursor approaches the target, the uncertainty in the user's intended endpoint shrinks. When the cursor is far from the target, σ_t is large and the distribution overlaps weakly with the target.

The target itself defines a fixed "null" Gaussian:

$$p_0(x) = \mathcal{N}\big(x_{\text{target}}, \sigma_0^2 I\big)\,, \qquad \sigma_0 = R,$$

where R is the physical target radius in the task. The relationship between p_t and p_0 quantifies moment-by-moment changes in the user's progress.

4.2 Entropy and Instantaneous Information Gain

For an isotropic d-dimensional Gaussian, the differential entropy is

$$H = \frac{1}{2}\log\big[(2\pi e)^d \sigma^2\big]\,.$$

Let H_t denote the entropy of the cursor-induced distribution at time t, and let H_0 be the constant entropy of the target. Between frames $t - \Delta t$ and t, the instantaneous information gain is defined as:

$$\Delta I_t = H_{t-\Delta t} - H_t.$$

This quantity has desirable behavioral structure:

- $\Delta I_t > 0$: the cursor moved closer to the target (uncertainty decreases).
- $\Delta I_t < 0$: the cursor moved away from the target (uncertainty increases).
- $\Delta I_t = 0$: curvature or tangential motion that does not reduce radial error.

The *total information transmitted* during the trial is the sum

$$I_{\text{trial}} = \sum_t \Delta I_t,$$

and dividing by trial duration T yields the throughput estimate:

$$TP = \frac{I_{\text{trial}}}{T} \quad \text{(bits/s)}.$$

4.3 Concrete Javascript Parameterization

Our implementation uses the following concrete mapping, consistent with the frame-level data logged in the experiments analyzed in Section 4 :contentReference[oaicite:1]index=1:

- Target radius R is taken directly from the task configuration.
- Cursor–target distance r_t is computed per frame as

$$r_t = \sqrt{(x_t - x_{\text{target}})^2 + (y_t - y_{\text{target}})^2}.$$

- Frame-wise entropy follows:

$$H_t = \tfrac{1}{2} \log\left[(2\pi e)^2 \, r_t^2\right]$$

  in the 2D task.

- Information increments are accumulated in real time at 120 Hz.

Because entropy depends *only on distance*, the metric is invariant to curvature, hand path shape, and instantaneous cursor velocity. It purely reflects uncertainty reduction relative to the target prior.

4.4 Application: Click vs. Hold Endpoint Confirmation

Figure 1 illustrates an application of this entropy-based throughput measure, comparing two task variants that differ only in how the endpoint is confirmed:

1. **Click acquisition**: a discrete confirmation event.
2. **Hold acquisition**: the cursor must remain inside the target for a fixed dwell duration.

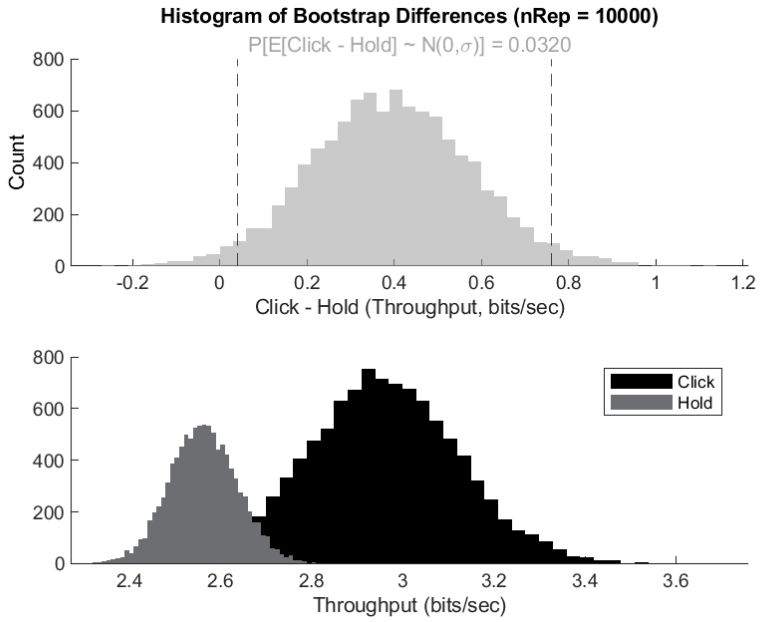

Figure 1: **Comparison of entropy–based throughput for Click vs. Hold endpoint confirmation.** Top: bootstrap distribution ($n = 10{,}000$ resamples) of the throughput difference Click − Hold, showing a clear positive shift indicating higher effective information transmission when acquisition is confirmed by a discrete click. Bottom: empirical throughput distributions for the two conditions, illustrating that the Hold requirement prolongs trial duration without contributing additional uncertainty reduction, thereby reducing bits/s under the Gaussian–entropy model.

Although the motor trajectories appear similar qualitatively, the entropy trajectory differs: click-based confirmation allows fast "commitment" once the cursor stabilizes at the endpoint, whereas the hold condition extends trial duration without contributing additional uncertainty reduction. Because the entropy-based throughput explicitly divides accumulated information by elapsed time, the hold condition yields a systematically lower bit rate.

This is visible in the bootstrap distributions, where the mean throughput for the click condition exceeds the hold condition by approximately 0.3–0.5 bits/s in pilot data. Importantly, this difference emerges naturally from the information model and does not require fitting movement-time regressions or estimating nominal target widths.

4.5 Advantages Over Classical Throughput

This formulation has several methodological benefits:

- **Continuous evaluation**: does not require identifying ballistic vs. corrective submovements [13].
- **Signed information**: penalizes overshoot and backtracking automatically.
- **Geometry-agnostic**: does not require explicit measurement of D or W, which is helpful in irregular or adaptive target layouts.
- **Endpoint-neutral**: works with click, dwell, gesture, EMG-triggered, or neural-decoded selection.
- **Directly comparable across devices**: the output is in canonical bits/s.

Because the approach derives strictly from Shannon entropy and Gaussian approximations, it generalizes smoothly to other modalities (e.g. BCI cursor control or EMG-based pointing), where endpoint jitter or noisy neural decoding violates assumptions underlying classical effective-width formulations.

4.6 Relation to Broader Models of Motor Information

The Gaussian-entropy cursor model sits between classical Fitts formulations [8, 17] and modern optimal-control descriptions [**?**]. Like the rate–distortion interpretations of aimed movement [**?**], it treats movement as a sequence reducing task uncertainty. Unlike endpoint-only analyses, however, it measures *process information*, reflecting the full temporal evolution of the cursor.

This allows us to estimate differences in movement efficiency arising purely from task design (click vs. hold), encoder noise (EMG vs. mouse), or interface constraints, even when movement-time regressions or classical indices of difficulty are not appropriate.

5 Conclusion

The studies summarized in Table 8 emphasize a growing disconnect between existing throughput metrics and the behaviors that advanced neuroprosthetic systems ultimately seek to restore. Classical Fitts-style estimators measure information transfer in terms of discrete, endpoint-defined movements; this framework works well for pointing tasks, typing interfaces, or any setting in which a user selects from a finite and well-defined alphabet of choices. In contrast, the functional 3D behaviors demonstrated in the landmark studies of Hochberg et al. and Ajiboye et al. involve continuous trajectories, variable goals, and context-dependent optimization criteria. Such tasks do not admit simple definitions of target width or index of difficulty, and therefore cannot be evaluated using standard throughput measures.

A promising direction for quantifying these richer behaviors is the use of *transfer entropy* and related measures of directed information flow. Rather than requiring predefined targets, transfer entropy captures how much the user's

Study	Modality	DOF	TP (bits/s)
Hochberg et al. (2012)	Intracortical BCI, reach-and-grasp, multidimensional functional tasks	3D+	N/A
Ajiboye et al. (2017)	Intracortical BCI with FES, whole-arm functional movements	3D+	N/A

Table 8: Seminal intracortical BCI studies demonstrating high-degree-of-freedom functional movements, including grasp, reach, and multi-joint limb coordination. Although these works represent major scientific and translational milestones, they do not include the geometric manipulations (e.g., target widths, distances) required for classical or generalized throughput computation. Future analyses will require information-theoretic metrics that extend beyond discrete targets to quantify continuous, multidimensional motor intent in 3D space.

neural activity reduces uncertainty in the observed movement trajectory. For continuous-control BCIs, this provides a natural way to quantify the moment-by-moment information contribution of the user to the evolving system state. However, the approach still requires a shared probabilistic model of the task—a "common prior"—that specifies what counts as a meaningful deviation from chance. For point-to-point reaching, such priors can be constructed; for complex object manipulation or multi-step functional tasks, they remain an open research problem.

This notion of a shared prior also clarifies why throughput in typing interfaces can far exceed that of motor point-to-point tasks. The English language provides a deeply structured symbol space, allowing users to transmit information at dozens of bits per second by exploiting statistical regularities of words and phrases. In this sense, a keyboard is not merely a motor interface but a compression scheme: mutual information between intended and produced character streams is high because both sender and receiver share the same underlying linguistic model. The richness of the prior is what enables high throughput.

For expressive motor behaviors such as those observed in the carefully-practiced movements of a concert pianist, capable of invoking sorrow, inspiration, or simply tickling the imagination, the prior itself is unclear. Neither a saxophonist's subtle variation in timing or force, nor a painter's idiosyncratic brushstroke, maps cleanly onto a finite alphabet. Without an agreed-upon symbolic structure, information-theoretic throughput becomes fundamentally ill-defined. In such domains, the motor system is not merely transmitting discrete symbols but generating high-dimensional signals whose meaning emerges from shared human experience, cultural context, or aesthetics rather than measurable reductions in uncertainty.

As technology for digital input advances ever forward in enabling naturalis-

tic, expressive forms of digital interaction, the field must move beyond classical throughput and develop new measures that can capture the fluidity, nuance, and communicative depth of human motor behavior. Transfer entropy and continuous-state information metrics offer a mathematically principled starting point, but fully quantifying the richness of human action, from functional reach-to-grasp to the expressive capacity of a musician or artist, remains one of the central conceptual challenges for next-generation body-machine-interface evaluation.

6 Appendix

Continuous-Time Information Throughput

Pointing performance is quantified using an entropy-reduction formulation motivated by the discrete information-transfer framework of Wolpaw et al. [23] and the two-dimensional extension of Fitts' law developed by MacKenzie and Buxton [18].

Uncertainty model. At every rendered frame the cursor's positional uncertainty is modelled as a one-dimensional Gaussian with standard deviation

$$\sigma_t = \max(\sigma_{\min},\ s\, d_t)\,, \tag{31}$$

where d_t is the Euclidean cursor-to-target distance (pixels), s is a scale factor (default $s = 1$), and $\sigma_{\min}$ is a lower bound (default $\sigma_{\min} = 1\,\text{px}$) that prevents the entropy from diverging as $d_t \to 0$.

Entropy and per-frame information. The differential entropy of this Gaussian (bits) is

$$H_t = \tfrac{1}{2}\log_2\!\left(2\pi e\,\sigma_t^2\right), \tag{32}$$

and the information gained during frame t equals the entropy reduction:

$$I_t = H_{t-1} - H_t \quad \text{(bits)}. \tag{33}$$

Negative values arise when the cursor moves away from the target and are retained in the accumulation, so inefficient trajectories reduce the total.

Cumulative information and leg-average throughput. Cumulative information is accumulated over all N frames of each movement leg (OUTBOUND or INBOUND):

$$B_N = \sum_{t=1}^{N} I_t = H_0 - H_N = \log_2 \frac{\sigma_0}{\sigma_N}, \tag{34}$$

where the telescoping equality holds exactly. The per-leg throughput reported in the exported trial data is the leg-average bits per second:

$$\text{ITR} = \frac{B_N}{T_N} \quad \left(\text{bits}\,\text{s}^{-1}\right), \tag{35}$$

with T_N denoting the total leg duration. An exponential moving average (EMA) with smoothing factor $\alpha = 0.25$ is maintained separately for display purposes only and is not used as the primary throughput estimate.

Relation to classical Fitts throughput. At the start of a leg the cursor is at the source target, so $\sigma_0 = s\, d_0$ where d_0 is the centre-to-centre movement amplitude D. At acquisition $d_N \leq r$ (target radius), so $\sigma_N \approx s\, r \propto W/2$ where W is the target diameter. Substituting into (34) gives

$$B_N \approx \log_2 \frac{D}{W/2} = \log_2 \frac{2D}{W}, \tag{36}$$

which is MacKenzie's formulation of Fitts' index of difficulty [17]. Dividing by movement time T_N recovers the classical throughput TP = ID/MT. The connection to Wolpaw et al. [23] follows by treating the workspace as a uniform grid of $N \propto (D/W)^2$ equiprobable cells, whose prior entropy $\log_2 N \approx 2\, B_N$ mirrors Wolpaw's $\log_2 N$ baseline term; the cross-entropy between this uniform prior and the Gaussian endpoint density then reduces to (36) [18].

References

[1] Ali Ameri, Mohammad Ali Akhaee, Erik Scheme, and Kevin Englehart. Real-time, simultaneous myoelectric control using a convolutional neural network. *PLOS ONE*, 13(9):e0203835, 2018. doi: 10.1371/journal.pone.0203835.

[2] B. S. Atal and S. L. Hanauer. Speech analysis and synthesis by linear prediction of the speech wave. *The Journal of the Acoustical Society of America*, 50(2B):637–655, 1971. doi: 10.1121/1.1912673.

[3] Bishnu S. Atal and Manfred R. Schroeder. Predictive coding of speech signals. *Bell System Technical Journal*, 49(8):1973–1986, 1970. doi: 10.1002/j.1538-7305.1970.tb01719.x.

[4] Rachael A. Burno, Bing Wu, Rina Doherty, Hannah Colett, and Rania Elnaggar. Applying fitts' law to gesture-based computer interactions. *Procedia Manufacturing*, 3:4342–4349, 2015. doi: 10.1016/j.promfg.2015.07.429.

[5] Stuart K. Card, William K. English, and Betty J. Burr. Evaluation of mouse, rate-controlled isometric joystick, step keys, and text keys for text selection on a crt. *Ergonomics*, 21(8):601–613, 1978. doi: 10.1080/00140137808931762.

[6] Cynthia A Chestek et al. Neural control of 3d reaching with utah arrays. *Journal of Neural Engineering*, 9(4):046014, 2012. doi: 10.1088/1741-2560/9/4/046014.

[7] Elizabeth A. Felton, John C. Williams, James A. Wilson, and Paula C. Garell. Applying fitts' law to a brain–computer interface. *Journal of Neural Engineering*, 6(5):056002, 2009. doi: 10.1088/1741-2560/6/5/056002.

[8] Paul M. Fitts. The information capacity of the human motor system in controlling the amplitude of movement. *Journal of Experimental Psychology*, 47(6):381–391, 1954. doi: 10.1037/h0055392.

[9] A. Gray and L. Markel. Distance measures for speech processing. *IEEE Transactions on Acoustics, Speech, and Signal Processing*, 24(5):380–391, 1976. doi: 10.1109/TASSP.1976.1162830.

[10] Robert M. Gray and John C. Kieffer. Mutual information, rate distortion, and quantization in metric spaces. *IEEE Transactions on Systems, Man, and Cybernetics*, 10(3):146–156, 1980. doi: 10.1109/TSMC.1980.4308731.

[11] J Gusman et al. Evaluation of computer-based target achievement with myoelectric input. *Biomedical Engineering Online*, 16(31), 2017. doi: 10.1186/s12938-017-0354-1.

[12] John Paulin Hansen, Vinay Rajanna, I. Scott MacKenzie, and Per Baekgaard. Gaze + point: Modeling gaze and controller input for 2d pointing in vr. In *Proceedings of the 2018 CHI Conference on Human Factors in Computing Systems*, pages 1–12, 2018. doi: 10.1145/3173574.3173790.

[13] Errol R. Hoffman and Donald E. Meyer. Submovements, movement variability, and speed-accuracy tradeoff in rapid fingertip aiming. *Journal of Experimental Psychology: Human Perception and Performance*, 9(4):765–778, 1983. doi: 10.1037/0096-1523.9.4.765.

[14] Daomu Huang et al. A hybrid bci based on visual tracking and eeg. *Neural Networks*, 102:11–19, 2018. doi: 10.1016/j.neunet.2018.01.002.

[15] Peter J Ifft, Mikhail A Lebedev, and MAL Nicolelis. Cortical correlates of fitts' law. *Frontiers in Integrative Neuroscience*, 5:85, 2011. doi: 10.3389/fnint.2011.00085.

[16] Sung-Phil Kim, John D. Simeral, Leigh R. Hochberg, John P. Donoghue, and Michael J. Black. Point-and-click cursor control with an intracortical neural interface system by humans with tetraplegia. *IEEE Transactions on Neural Systems and Rehabilitation Engineering*, 19(2):193–203, 2011. doi: 10.1109/TNSRE.2011.2107750.

[17] I. Scott MacKenzie. Fitts' law as a research and design tool in human–computer interaction. In *Proceedings of the SIGCHI Conference on Human Factors in Computing Systems*, pages 349–354, 1992. doi: 10.1145/142750.142794.

[18] I. Scott MacKenzie and William Buxton. Extending Fitts' law to two-dimensional tasks. In *Proceedings of CHI '92*, pages 219–226. ACM, 1992.

[19] C Matlack et al. Empirical movement models for brain–computer interfaces. *IEEE Transactions on Neural Systems and Rehabilitation Engineering*, 24 (5):534–544, 2016. doi: 10.1109/TNSRE.2016.2545641.

[20] Alan McCree and Thomas P. Barnwell. A mixed excitation lpc vocoder model for low bit rate speech coding. *IEEE Transactions on Speech and Audio Processing*, 3(4):242–250, 1995. doi: 10.1109/89.388902.

[21] Manfred R. Schroeder and Bishnu S. Atal. Code-excited linear prediction (celp): High-quality speech at very low bit rates. *ICASSP '85. IEEE International Conference on Acoustics, Speech, and Signal Processing*, pages 937–940, 1985. doi: 10.1109/ICASSP.1985.1168513.

[22] Ping Wang et al. Volitional ecog control of 3d movement. *Journal of Neuroscience*, 33(14):5937–5946, 2013. doi: 10.1523/JNEUROSCI.4983-12.2013.

[23] Jonathan R. Wolpaw, Niels Birbaumer, Dennis J. McFarland, Gert Pfurtscheller, and Theresa M. Vaughan. Brain-computer interfaces for communication and control. *Clinical Neurophysiology*, 113(6):767–791, 2002.

[24] Sophie M. Wurth and Levi J. Hargrove. A real-time comparison between direct control, sequential pattern recognition control and simultaneous pattern recognition control using a fitts' law style assessment procedure. *Journal of NeuroEngineering and Rehabilitation*, 11(1):91, 2014. doi: 10.1186/1743-0003-11-91.

[25] Xiaojun Zhang, Anders Markussen, Jacob O. Wobbrock, and Kasper Hornbæk. Text entry throughput: Towards unifying speed and accuracy in a single metric. In *Proceedings of the 2019 CHI Conference on Human Factors in Computing Systems*, pages 1–13, 2019. doi: 10.1145/3290605.3300613.